Simulation Modelling Practice and Theory 109 (2021) 102235

Contents lists available at ScienceDirect

Simulation Modelling Practice and Theory

journal homepage: www.elsevier.com/locate/simpat

Trajectory tracking control of steer-by-wire autonomous ground vehicle considering the complete failure of vehicle steering motor

Te Chen, Yingfeng Cai, Long Chen *, Xing Xu *, Xiaoqiang Sun

Automotive Engineering Research Institute, Jiangsu University, Zhenjiang 212013, China

ARTICLE INFO

Keywords:
Autonomous ground vehicles
Trajectory tracking
Differential steering
Motor fault
Sliding mode control
Observer design

ABSTRACT

This paper investigates the trajectory tracking control problem of steer-by-wire autonomous ground vehicle considering the complete failure of vehicle steering motor. In order to achieve the trajectory tracking control of autonomous ground vehicle in presence of the complete failure of vehicle steering motor, the mechanical transmission mechanism of vehicle steering system is analyzed with the steering motor fault being considered, and the differential steering is used to actuate the turning of vehicle in case of emergency. A model predictive controller with the constraints of tire cornering angle and road adhesion is designed to compute the expected front-wheel steering angle for vehicle trajectory tracking control, and a nonsingular terminal sliding mode controller is proposed to track the expected front-wheel steering angle using differential-steering moment, in which a novel observer design method is presented to estimate the actual front-wheel steering angle. Two case studies are implemented in a CarSim-Simulink co-simulation platform, and the simulation results have verified that the proposed method have satisfactory trajectory tracking control effectiveness in presence of the complete failure of vehicle steering motor.

1. Introduction

In recent decades, the development and progress of society has contributed to the overall technical level and popularity of the automobile industry [1-3]. Intelligent vehicles can effectively improve the road utilization rate of vehicles and passenger comfort, and reduce the potential road traffic risks [4-5]. The autonomous control ability of vehicles also meets the increasing demand of current consumers for driving and riding [6-7]. It is one of the major development directions in the field of vehicle control. The intelligent control technology of autonomous ground vehicle benefits from the maturity and popularization of vehicle electronic control technology [8-10], and the increasingly perfect supply channel of parts and components from the middle and lower reaches also provide a reliable guarantee for the development and expansion of the entire industrial chain [11-14]. Recently, it has received unprecedented attention and research and development investment from researchers and many manufacturers. Trajectory tracking (TT) control is a common scene in driverless driving process of autonomous vehicle. In the process of trajectory tracking, the trajectory tracking error and heading error is aimed to be reduced in real time through the steering motion control of the vehicle [15-17], so as to approach the referenced trajectory, and in order to solve the trajectory tracking problem in different situations, there are many related research results at present [18-23].

In the trajectory-tracking process of autonomous ground vehicle, vehicle steering control is the direct factor to guide autonomous

* Corresponding author.
E-mail addresses: chenlong@ujs.edu.cn (L. Chen), xuxing@mail.ujs.edu.cn (X. Xu).

https://doi.org/10.1016/j.simpat.2020.102235
Received 6 February 2020; Received in revised form 29 October 2020; Accepted 22 November 2020
Available online 24 November 2020
1569-190X/

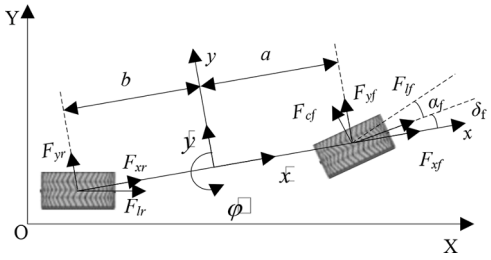

Fig. 1. Vehicle trajectory tracking model.

vehicle to track the referenced trajectory. Therefore, the accuracy and reliability of vehicle steering control directly affect the effect of trajectory tracking. In this case, the steer-by-wire system has attracted the attention of researchers with its unique advantages, and has become one of the recognized solutions in the field of unmanned vehicle steering control. In the steer-by-wire system, part of the mechanical connection between the hand steering wheel and the front-wheel of the vehicle has been cancelled, so that this mechanical driving structure can get rid of various limitations of the traditional steering system, which is conducive to further improving the maneuverability, comfort and safety of the vehicle [24-27]. The technology of steer-by-wire realizes the decoupling of driver's operation and vehicle's movement, which is helpful to improve the accuracy of steering control and the safety of passengers in the face of emergency [28]. The steer-by-wire system of vehicle adopts the direct torque drive by steering motor control to realize the vehicle steering, this advantage makes it easier to communicate and integrate with other active safety control subsystems of the vehicle, so as to provide a good hardware basis for autonomous steering of unmanned ground vehicles [29-31]. Based on the above considerations, steer by wire system is recognized as one of the key components and effective solutions to achieve advanced automatic driving at present. Therefore, the related research of steer-by-wire system and its integrated application on autonomous vehicle become the research hotspot in the field of vehicle intelligent control technology.

However, once the steer-by-wire system fails, the above-mentioned control advantages will no longer exist, and the control performance of autonomous ground vehicles will not be guaranteed, and even great risks may occur. Therefore, highly intelligent and autonomous capability is one of the important directions of the development of unmanned ground vehicles [32-35], and the adaptability to multiple working conditions and the control regulation ability in case of emergency is one of the important ways to improve the ability of vehicle autonomous control [36-39]. In the process of vehicle trajectory tracking, if the steering motor of vehicle fails completely, it is difficult for the existing control methods to make appropriate fault-tolerant control behavior for the emergency. The research on this problem in the existing literature is also insufficient, and this problem has great research necessity and practical application value. For this situation, considering the complete failure of vehicle steering motor, the mechanical transmission mechanism of vehicle steering system is analyzed and the dynamic equation of vehicle system is derived with the motor fault being considered, in which the differential steering moment is used to impel the vehicle to steer as required in case of emergency.

According to the above problem description, an overall control strategy for trajectory tracking control of autonomous vehicle is designed, in which a model predictive controller (MPC) is developed to obtain the expected front-wheel steering angle, and a non-singular terminal sliding mode controller (NTSMC) is designed to track the expected front-wheel steering angle by vehicle differential steering. The main contributions of this paper are summarized as follows: (a) a novel problem description for vehicle steering control is investigated, in which the mechanism of vehicle differential steering and its influence on vehicle steering movement is studied; (b) a more all-round overall vehicle trajectory tracking control strategy is presented, including trajectory tracking control and front-wheel steering angle tracking control; (c) considering that the actual front-wheel steering angle is hard to be measured directly, a novel front-wheel steering angle estimator is proposed using the design method of unknown input observer (UIO).

The rest of this paper is organized as follows. The background and related works are presented is Section 2. The trajectory tracking control method is shown in Section 3. The simulation results are provided in Section 4, followed by the conclusion in Section 5.

2. Background and related works

2.1. Vehicle trajectory tracking model

The vehicle trajectory tracking model [40] is shown in Figure 1. The influence of air resistance and suspension system on vehicle dynamics is not considered, only the motion of vehicle on horizontal plane is considered. In the trajectory-tracking dynamics model of Figure 1, the vehicle centroid coincides with the origin of the coordinate system *oxy*, in which the forward direction of *x*-axis denotes the vehicle heading direction, the forward direction of *y*-axis denotes the transverse direction of vehicle body. The coordinate system *OXY* represents the geodetic coordinate system. The vehicle dynamics equations along *x* axis, *y* axis and around *z* axis can be expressed as

$$m\ddot{x} = m\dot{y}\dot{\varphi} + 2F_{xf} + 2F_{xr} \tag{1}$$

$$m\ddot{y} = -m\dot{x}\dot{\varphi} + 2F_{yf} + 2F_{yr} \tag{2}$$

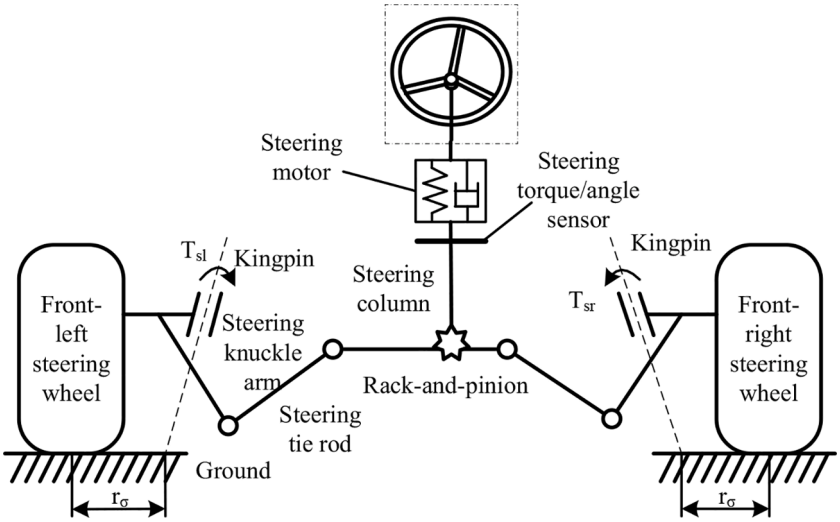

Fig. 2. Vehicle steering system model.

$$I_z\ddot{\varphi} = 2aF_{yf} - 2bF_{yr} \tag{3}$$

where m is the vehicle mass, a is the distance between vehicle mass center and front axle, b is the distance between vehicle mass center and rear axle, I_z stands for the moment of inertia, $\varphi$is the heading angle of vehicle, F_{xf} and F_{xr} is the tire force along the x axis of front tire and rear tire, respectively, F_{yf} and F_{yr} is the tire force along the y axis of front tire and rear tire, respectively. Assume that the tire forces of autonomous vehicle work in the linear region, then, the tire force can be written as

$$\begin{cases} F_{xf} = C_{lf}s_f \\ F_{xr} = C_{lr}s_r \end{cases} \tag{4}$$

$$\begin{cases} F_{yf} = C_{cf}\alpha_f \\ F_{yr} = C_{cr}\alpha_r \end{cases} \tag{5}$$

where C_{lf} and C_{lr} is the longitudinal tire stiffness of front tire and rear tire, respectively, s_f and s_r is the tire slip rate of front tire and rear tire, respectively, C_{cf} and C_{cr} is the tire cornering stiffness of front tire and rear tire, respectively, α_f and α_r is the tire slip angle of front and rear tire, respectively. And the tire slip angle can be written as

$$\begin{cases} \alpha_f = \delta_f - \dfrac{a\dot{\varphi} + \dot{y}}{\dot{x}} \\ \alpha_r = \dfrac{b\dot{\varphi} - \dot{y}}{\dot{x}} \end{cases} \tag{6}$$

where δ_f is the steering angle of front wheels. Combining equation (1), (2), (3), with (4), (5), (6), the vehicle dynamics model in trajectory tracking control can be obtained as

$$\begin{cases} m\ddot{x} = m\dot{y}\dot{\varphi} + 2\left[C_{lf}s_f - C_{cf}\left(\delta_f - \dfrac{a\dot{\varphi} + \dot{y}}{\dot{x}}\right)\delta_f + C_{lr}s_r\right] \\ m\ddot{y} = -m\dot{x}\dot{\varphi} + 2\left[C_{lf}s_f\delta_f + C_{cf}\left(\delta_f - \dfrac{a\dot{\varphi} + \dot{y}}{\dot{x}}\right) + C_{cr}\dfrac{b\dot{\varphi} - \dot{y}}{\dot{x}}\right] \\ I_z\ddot{\varphi} = 2a\left[C_{lf}s_f\delta_f + C_{cf}\left(\delta_f - \dfrac{a\dot{\varphi} + \dot{y}}{\dot{x}}\right)\right] - 2bC_{cr}\dfrac{b\dot{\varphi} - \dot{y}}{\dot{x}} + M_z \end{cases} \tag{7}$$

where M_z is the external yaw moment of vehicle. The vehicle coordinates in the geodetic coordinate can be denoted as

$$\begin{cases} \dot{Y} = \dot{x}\sin\varphi + \dot{y}\cos\varphi \\ \dot{X} = \dot{x}\cos\varphi - \dot{y}\sin\varphi \end{cases} \tag{8}$$

2.2. Vehicle steering system model

The rack-and-pinion steer-by-wire system [41-42] of autonomous vehicle is shown is Figure 2. In the steer-by-wire system, there is no direct mechanical connection between the steering wheel and the vehicle steering system. For autonomous ground vehicles, the

hand steering wheel is no longer required. Therefore, the steering system of autonomous vehicle can control the steering motor to achieve front wheel steering according to the trajectory tracking requirements in the intelligent driving scenario. The driving torque of steering motor actuates the rack and pinion through the steering column, and the dynamics equation from the steering motor to rack and pinion can be written as

$$J_{sm}\ddot{\theta}_s + C_{sm}\dot{\theta}_s + K_{sm}\theta_s = T_m + \tau_{sg} + \tau_f \tag{9}$$

where J_{sm} is the moment of inertia of steering column, θ_s is the steering angle of steering column, C_{sm} is the damping of steering column system, K_{sm} is the stiffness of steering column, T_m is the driving torque of steering motor,$\tau_{sg}$is the reaction torque of steering trapezoidal system acting on gear, $\tau_f$is the steering system friction torque from rack and pinion. The rotational torque of steering column will drive the tie rod through the movement of rack and pinion. The movement of tie rod is transmitted through the steering trapezoid to drive the front-wheel steering motion of vehicle. The dynamic equation from steering pinion to steering trapezoidal system is expressed as

$$J_{fm}\ddot{\delta}_f + C_{fm}\dot{\delta}_f + K_{fm}\delta_f = \tau_z + T_s + \tau_{gs} \tag{10}$$

where J_{fm} is the moment of inertia of steering trapezoidal system, C_{fm} is the damping of steering trapezoidal system, K_{fm} is the stiffness of steering trapezoidal system, $\tau_z$is the tire aligning torque,$\tau_{gs}$is the torque of steering column acting on rack and pinion, T_s is the moment difference of the kingpin between the front two wheels. According to Newton's third law, the forces and reactions are opposite to each other. Thus, the transmission ratio of steering gear is denoted as k_s, we have $k_s\tau_{sg} + \tau_{gs} = 0$. Combing equation (9) with equation (10), the equivalent dynamics equation of vehicle steering system can be obtained as

$$J_{eq}\ddot{\delta}_f + C_{eq}\dot{\delta}_f + K_{eq}\delta_f = k_s T_m + k_s\tau_f + \tau_z + T_s \tag{11}$$

where J_{eq} is the equivalent inertia moment of steering system which can be written as$J_{eq} = J_{fm} + k_s^2 J_{sm}$, C_{eq} is the equivalent rotational damping of steering system which can be written as $C_{eq} = C_{fm} + k_s^2 C_{sm}$, K_{eq} is the equivalent rotational stiffness of steering system which can be written as $K_{eq} = K_{fm} + k_s^2 K_{sm}$.

The differential steering (DS) system can rely on the torque difference between the front two wheels to drive the steering system to rotate [43-45]. The difference in drive torque between the front left and right wheels causes the front left and right wheels of the vehicle to rotate around their respective kingpins. Due to the existence of the steering trapezoid mechanism in the vehicle steering system [46], this torque difference will force the steering trapezoid mechanism to turn to the side with less driving torque, so as to drive the vehicle steering system to start steering action, and realize the steering demand of the unmanned vehicle. In this way, the vehicle differential steering mechanism can be used as a backup mechanism for vehicle steering by wire [47-49]. When the vehicle steer-by-wire motor fails completely, the differential steering mechanism can be activated to realize the vehicle steering requirements urgently, so as to improve the decision-making and fault-tolerance ability of the autonomous vehicle in the face of unknown risks [50-51].

3. Trajectory tracking control method

3.1. Problem description and overall control strategy

The complete failure of steering motor is considered in this paper. When the steering motor fails completely, the torque transmitted by steering motor to steering column is considered as 0. As shown in Figure 2, the driving force of front-left and front-right wheel will generate a moment with the kingpin as the rotation axis. When the driving forces of the left and right wheels are different, this moments are different, and the generated moment difference will actuate the vehicle to turn through the steering trapezium system. The moment difference of the kingpin between the front two wheels can be given by

$$T_s = \left(F_{xfr} - F_{xfl}\right) r_\sigma \tag{12}$$

where$r_\sigma$is the kingpin lateral offset which represents the distance between the projection point of the kingpin on the ground and the central plane of the tire, $F_{xfr}$and F_{xfl}represents the longitudinal tire force of front-right and front-left wheel, respectively. The vehicle yaw moment generated by differential moment can be expressed as

$$M_z = \left(F_{xfr} - F_{xfl}\right) l_d \tag{13}$$

where$M_z$is the yaw moment, $l_d$is the half wheelbase. According to equation (12) and equation (13), we have$T_s = \frac{r_\sigma}{l_d} M_z$. Therefore, in case of complete failure of the steering motor, the equation (11) can be rewritten as

$$J_{eq}\ddot{\delta}_f + C_{eq}\dot{\delta}_f + K_{eq}\delta_f = k_s\tau_f + \tau_z + \frac{r_\sigma}{l_d} M_z \tag{14}$$

According to equation (14), one can find that the differential torque between the two front wheels will help the vehicle to steer.

The expected front-wheel steering angle obtained by MPC-based trajectory tracking controller is denoted asδ_{fd}. Defining that$x_1 = \delta_f - \delta_{fd}$, $x_2 = \dot{\delta}_f$, and according to equation (14), the state space equation of steering system can be written as

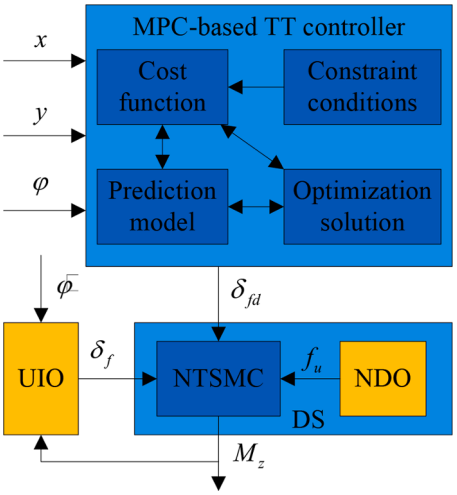

Fig. 3. Overall control strategy.

$$\begin{cases} \dot{x}_1 = x_2 \\ \dot{x}_2 = f(x) + b_u u + f_u \end{cases} \tag{15}$$

where$f(x) = -\frac{K_{eq}}{J_{eq}}x_1 - \frac{C_{eq}}{J_{eq}}x_2, b_u = \frac{r_a}{J_{eq}l_d}, u = M_z$represents the control input,$f_u = \frac{1}{J_{eq}}(k_s\tau_f + \tau_z - K_{eq}\delta_{fd})$represents the system interference. Thus, it can be found that the control target is to design the optimal control item of $M_z$to make the system converge to 0 in finite time, which helps the actual front-wheel steering angle approach to the expected front-wheel steering angle during the trajectory tracking process.

The overall control strategy is shown in Fig. 3. The MPC-based trajectory tracking controller calculates the expected front-wheel steering angle according to the trajectory tracking requirements. Considering that the actual front-wheel steering angle of vehicle is difficult to be measured directly, an unknown input observer is designed to estimate the front-wheel steering angle, and the estimated result is used as the input of vehicle steering controller. In presence of the complete failure of vehicle steering motor, a nonsingular terminal sliding mode control method is proposed to track the expected front-wheel steering angle by vehicle differential steering.

3.2. MPC-based TT controller

The linear time-varying equation of equation (7) can be expressed as

$$\begin{aligned} \dot{\xi}_t &= f(\xi_t, u_t) = A_t\xi_t + B_t u_t \\ y &= C\xi_t \end{aligned} \tag{16}$$

where the system state vector is$\xi_t = \begin{bmatrix} \dot{x} & \dot{y} & \varphi & \dot{\varphi} & Y & X \end{bmatrix}^T$, the control input is$u_t = \delta_f, A_t = \frac{\partial f}{\partial \xi}$is the state transition matrix, $B_t = \frac{\partial f}{\partial u}$is the input matrix, and$C = \begin{bmatrix} 0 & 0 & 0 & 0 & 1 & 0 \\ 0 & 0 & 1 & 0 & 0 & 0 \end{bmatrix}$is the measurement matrix. Then, the discrete equation of (16) can be written as

$$\begin{cases} x(k+1|k) = \widetilde{A}_k\xi(k|k) + \widetilde{B}_k\Delta u(k|k) \\ \eta(k|k) = \widetilde{C}(k)x(k|k) \end{cases} \tag{17}$$

where$x(k|k) = [\xi(k|k) \quad u(k-1|k)]^T, \widetilde{A}(k) = \begin{bmatrix} A(k) & B(k) \\ 0_{1\times 6} & 1 \end{bmatrix}, \widetilde{B}(k) = [B(k) \quad 1]^T, \widetilde{C}(k) = \begin{bmatrix} 0 & 0 & 0 & 0 & 1 & 0 \\ 0 & 0 & 1 & 0 & 0 & 0 \end{bmatrix}$.

According to equation (17), the model prediction equation of k sample time can be expressed as

$$Y(k+1|k) = \Psi_\xi\xi(k) + \Theta_\xi\Delta U(k) \tag{18}$$

where$Y(k+1|k)$is the system output at the k sample time, $\Delta U(k)$is the system input at the k sample time, and $Y(k+1|k) =$

$$\begin{bmatrix}\eta(k+1|k)\\ \eta(k+2|k)\\ \vdots\\ \eta(k+h_p|k)\end{bmatrix},\Delta U(k)=\begin{bmatrix}\Delta u(k)\\ \Delta u(k+1)\\ \vdots\\ \Delta u(k+h_c-1)\end{bmatrix},\Psi_\xi=\begin{bmatrix}C\widetilde{A}_{k,1}C\widetilde{A}_{k,2}\cdots C\widetilde{A}_{k,h_c}\cdots C\widetilde{A}_{k,h_p}\end{bmatrix}^T,\Theta_\xi=\begin{bmatrix}C\widetilde{B}_k & 0 & \cdots & 0\\ C\widetilde{A}_k\widetilde{B}_k & C\widetilde{B}_k & \cdots & 0\\ \vdots & \vdots & \ddots & \vdots\\ C\widetilde{A}_{k,h_c-1}\widetilde{B}_k & C\widetilde{A}_{k,h_c-2}\widetilde{B}_k & \cdots & C\widetilde{A}_k\\ C\widetilde{A}_{k,h_c}\widetilde{B}_k & C\widetilde{A}_{k,h_c-1}\widetilde{B}_k & \cdots & C\widetilde{A}_k\widetilde{B}_k\\ \vdots & \vdots & \ddots & \vdots\\ C\widetilde{A}_{k,h_p-1}\widetilde{B}_k & C\widetilde{A}_{k,h_p-1}\widetilde{B}_k & \cdots & C\widetilde{A}_{k,h_p-h_c-1}\widetilde{B}_k\end{bmatrix},$$ h_p is

the prediction horizon, h_c is the control horizon.

The cost function is designed as

$$J_M=\sum_{j=1}^{h_p}q_1\|\Delta\eta(k+j|k)\|^2+\sum_{j=0}^{h_c-1}q_2\|\Delta u(k+j|k)\|^2+q_3\varepsilon^2 \tag{19}$$

where$\Delta\eta(k+j|k)$is the tracking error between the actual system state and referenced system state, $\Delta u(k+j|k)$is the control increment consisting of front-wheel steering angle and external yaw moment, $\varepsilon$is the relaxation factor, q_1, q_2 $q_3$are the weight coefficients.

The constraint of tire cornering angle is expressed as$|\alpha_{f,r}|\leq 2^\circ$. The constraint of road adhesion is expressed as$a_{y,\min}-\varepsilon\leq a_y\leq a_{y,\max}+\varepsilon$, where$\mu_ganda_y$represents the road adhesion coefficient and lateral vehicle acceleration, respectively. Therefore, the optimization model of model predictive controller can be given by

$$\begin{cases}\min J_M\\ s.t.\Delta U_{\min}\leq\Delta U_t\leq\Delta U_{\max}\\ U_{\min}\leq A_U\Delta U_t+U_t\leq U_{\max}\\ y_{h,min}\leq y_h\leq y_{h,\max}\\ y_{s,min}-\varepsilon\leq y_s\leq y_{s,max}+\varepsilon\end{cases} \tag{20}$$

where$U_{\min}$and$U_{\max}$are the upper and lower boundary values of control input, $\Delta U_{\min}$and$\Delta U_{\max}$are the upper and lower boundary values of control input increment, $y_{h,min}$and$y_{h,\max}$are the upper and lower boundary values of hard constraint of output,$y_{s,min}$and$y_{s,\max}$are the upper and lower boundary values of soft constraint of output, $A_U$is the Kronecker product of an unit lower triangular matrix and an unit matrix.

3.3. Tracking control of front-wheel steering angle using NTSMC

In order to make the tracking error converge quickly and avoid singular problems effectively, the nonsingular terminal sliding mode control is used to design the nonlinear error feedback control law. According to the state space equation (20), the nonsingular fast terminal sliding surface is selected as

$$s=x_1+k_1x_2^{k_2} \tag{21}$$

where k_1 and k_2 are regulating parameters, $k_1>0$, $1<k_2=k_x/k_y<2$,$k_x$and$k_y$are positive odd numbers. The sliding mode control law can be written as

$$u=u_e+u_f \tag{22}$$

where$u_e$is the equivalent control item,$u_f$is the feedback control item. To make the system state approach to the sliding surface and converge to the desired state along the sliding surface in finite time, calculating the derivative of terminal sliding surface in equation (21), we have

$$\dot{s}=x_2+k_1k_2x_2^{k_2-1}(f(x)+b_uu+f_u) \tag{23}$$

By calculating $\dot{s}=0$, the equivalent control item can be obtained as

$$u_e=-\frac{1}{b_u}\left(\frac{x_2^{2-k_2}}{k_1k_2}+f(x)+f_u\right) \tag{24}$$

Then, in order to make the sliding motion approach to the sliding mode surface, the exponential approach law is chosen as$\dot{s}=-l_1s-l_2\mathrm{sgn}(s)$, and the feedback control item is designed as

$$u_f=-\frac{1}{b_u}(l_1s+l_2\mathrm{sgn}(s)) \tag{25}$$

where$l_1$and$l_2$are positive parameters. Combining the equation (24) and (25), the sliding mode control law can be expressed as

$$u = -\frac{1}{b_u}\left(\frac{x_2^{2-k_2}}{k_1 k_2} + f(x) + f_u + l_1 s + l_2 \mathrm{sgn}(s)\right) \tag{26}$$

According to equation (26), it can be found that the system interference f_u should be known to calculate the control item. Therefore, a nonhomogeneous disturbance observer (NDO) is developed to estimate the system interference.

$$\begin{cases} z_0 = v_0 + x_2 + k_1 k_2 x_2^{k_2-1} - f(x) - b_u u \\ v_0 = -\lambda_2 L^{\frac{1}{3}}(z_0 - s)^{\frac{2}{3}}\mathrm{sgn}(z_0 - s) - \mu_2(z_0 - s) + z_1 \\ z_1 = v_1 \\ v_1 = -\lambda_1 L^{\frac{1}{2}}(z_1 - v_0)^{\frac{1}{2}}\mathrm{sgn}(z_1 - v_0) - \mu_1(z_1 - v_0) + z_2 \\ z_2 = -\lambda_0 L \mathrm{sgn}(z_2 - v_1) - \mu_0(z_2 - v_1) \end{cases} \tag{27}$$

where $\lambda_{0,1,2}$ and $\mu_{0,1,2}$ are the positive constants. And the estimation of system interference is $\widehat{f}_u = z_1$.

To prove that the designed sliding mode control law can make the system converge to 0 in finite time, the Lyapunov function is chosen as $V = 0.5ss^T$. Calculating the derivative of Lyapunov function, we have

$$\begin{aligned} \dot{V} &= s\dot{s} = s\left(x_2 + k_1 k_2 x_2^{k_2-1}(f(x) + b_u u + f_u)\right) \\ &= s\left(x_2 + k_1 k_2 x_2^{k_2-1}\left(f(x) - \left(\frac{x_2^{2-k_2}}{k_1 k_2} + f(x) + f_u + l_1 s + l_2 \mathrm{sgn}(s)\right) + f_u\right)\right) \\ &= s\left(x_2 + k_1 k_2 x_2^{k_2-1}\left(-\frac{x_2^{2-k_2}}{k_1 k_2} - l_1 s - l_2 \mathrm{sgn}(s)\right)\right) \\ &= -k_1 k_2 x_2^{k_2-1}\left(l_1 s^2 + l_2 |s|\right) \end{aligned} \tag{28}$$

It known that $0 < k_2 - 1 < 1$, so $x_2^{k_2-1} \geq 0$. Thus, $\dot{V} \leq 0$ is satisfied, which indicates that the control system is stable.

3.4. Estimation of front-wheel steering angle based on UIO

It is difficult to measure the front-wheel steering angle of vehicle directly by using the on-board sensors. Therefore, it is necessary to design a model-based observer to estimate the front-wheel steering angle. The vehicle sideslip angle is defined as β, which can be obtained as $\beta = \arctan(\dot{y}/\dot{x}) \approx \dot{y}/\dot{x}$. Combining the vehicle sideslip angle with formula (5), (6), and (7), we have

$$\begin{cases} \ddot{\varphi} = -\dfrac{C_{cf}a^2 + C_{cr}b^2}{I_z \dot{x}}\dot{\varphi} + \dfrac{C_{cr}b - C_{cf}a}{I_z}\beta + \dfrac{C_{cf}a}{I_z}\delta_f + \dfrac{M_z}{I_z} \\ \dot{\beta} = -\left(1 + \dfrac{C_f a - C_r b}{m\dot{x}^2}\right)\dot{\varphi} - \dfrac{C_{cf} + C_{cr}}{m\dot{x}^2}\beta + \dfrac{C_f}{m\dot{x}}\delta_f \end{cases} \tag{29}$$

The state space equation of vehicle dynamics model with front-wheel steering angle in (29) is written as

$$\begin{cases} \dot{x}_v = Ax_v + Bu_v + Dd_v \\ y_v = Cx_v \end{cases} \tag{30}$$

where $x_v = [\dot{\varphi} \quad \beta]^T$ is the system state, $u_v = M_z$ is the system input, $d_v = \delta_f$ is the system unknown input, y_v is the system output, and the matrix A, B, C, D represents the state transition matrix, input matrix, measurement matrix, unknown input matrix, respectively. And the matrix A, B, C, D can be respectively expressed as $A = \begin{bmatrix} a_{11} & a_{12} \\ a_{21} & a_{22} \end{bmatrix}$, $B = [b_1 \quad 0]^T$, $C = \begin{bmatrix} 1 & 0 \\ 0 & 1 \end{bmatrix}$, $D = [b_2 \quad b_3]^T$, where $a_{11} = -\frac{C_{cf}a^2 + C_{cr}b^2}{I_z \dot{x}}$, $a_{12} = \frac{C_{cr}b - C_{cf}a}{I_z}$, $a_{21} = -\left(1 + \frac{C_f a - C_r b}{m\dot{x}^2}\right)$, $a_{22} = -\frac{C_{cf} + C_{cr}}{m\dot{x}^2}$, $b_1 = \frac{1}{I_z}$, $b_2 = \frac{C_{cf}a}{I_z}$, $b_3 = \frac{C_f}{m\dot{x}}$.

By observing the state space equation (30), one can find that the front-wheel steering angle to be estimated is the unknown input of system. Consequently, it is necessary to design a corresponding unknown input observer to estimate the front-wheel steering angle. To facilitate the design of UIO, a nonsingular matrix is designed as $T = [N \quad D] = \begin{bmatrix} 1 & b_2 \\ 1 & b_3 \end{bmatrix}$. Then, using the nonsingular matrix T, the state space equation (30) can be transformed into an observable canonical type and expressed as

$$\begin{cases} \dot{\bar{x}}_v = \overline{A}\bar{x}_v + \overline{B}u_v + \overline{D}d_v y_v = \overline{C}\bar{x}_v \end{cases} \tag{31}$$

Table 1
Vehicle parameters.

Symbol	Parameters	Value and units
m	Vehicle mass	800 kg
r	Effective radius of wheel	0.245 m
a	Distances from vehicle gravity center to the front axle	0.795 m
b	Distances from vehicle gravity center to the rear axle	0.975 m
l_d	Half treads of the front(rear) wheels	0.775 m
C_f	Equivalent cornering stiffness of front wheel	60000 N/rad
C_r	Equivalent cornering stiffness of rear wheel	40000 N/rad
I_z	Moment of inertia	1000 kg•m^2
J_{eq}	Equivalent inertia moment of steering system	0.1 kg•m^2
C_{eq}	Equivalent rotational damping of steering system	0.7 N•ms/rad
K_{eq}	Equivalent rotational stiffness of steering system	0.572 N•m/rad
k_s	Transmission ratio of steering gear	14.3
r_σ	Kingpin lateral offset	0.12 m

where$\overline{x}_v = T^{-1}x_v = \begin{bmatrix}\overline{x}_1 & \overline{x}_2\end{bmatrix}^T$,$\overline{A} = T^{-1}AT = \begin{bmatrix}\overline{a}_{11} & \overline{a}_{12}\\ \overline{a}_{21} & \overline{a}_{22}\end{bmatrix}$,$\overline{B} = T^{-1}B = \begin{bmatrix}\overline{b}_1 & \overline{b}_2\end{bmatrix}^T$,$C = CT = [CN \quad CD]$,$\overline{D} = T^{-1}D = [0 \quad 1]^T$.

By observing the transformed unknown input matrix$\overline{D}$, it can be found that one of the submatrices of system unknown input coefficient is 0, and the other submatrix is 1, which indicates that the unknown input of system can be decoupled by system model reduction. The decoupled subsystem can be given by

$$[I \quad 0]\dot{\overline{x}}_v = [\overline{a}_{11} \quad \overline{a}_{12}]\overline{x}_v + \overline{b}_1 u_v \tag{32}$$

$$[0 \quad I]\dot{\overline{x}}_v = [\overline{a}_{21} \quad \overline{a}_{22}]\overline{x}_v + \overline{b}_2 u_v + d_v \tag{33}$$

It can be found that the subsystem (32) is unknown-input-free. And the output equation can be expressed as

$$y_v = [CN \quad CD]\overline{x}_v \tag{34}$$

Choosing a nonsingular matrix as$U = \begin{bmatrix}b_2 & 0\\ b_3 & 1\end{bmatrix}$, then, its inverse matrix can be expressed as$U^{-1} = [U_1 \quad U_2]^T = \frac{1}{b_2}\begin{bmatrix}1 & 0\\ -b_3 & b_2\end{bmatrix}$. Through calculating, it can be obtained as$U_1CD = 1$and$U_2CD = 0$. MultiplyingU^{-1}at both sides of equation (26), we have

$$U_1 y_v = U_1 CN\overline{x}_1 + \overline{x}_2 \tag{35}$$

$$U_2 y_v = U_2 CN\overline{x}_1 \tag{36}$$

According to equation (32) and (35), we have

$$\dot{\overline{x}}_1 = \widetilde{A}_1\overline{x}_1 + \overline{b}_1 u_v + H_1 y_v \tag{37}$$

where$\widetilde{A}_1 = \overline{a}_{11} - \overline{a}_{12}U_1CN = \overline{a}_{11} - \frac{\overline{a}_{12}}{b_2}$,$H_1 = \overline{a}_{12}U_1 = \begin{bmatrix}\overline{a}_{12} & 0\end{bmatrix}$.

Then, combining equation (35) with (37), the observation equation of unknown input can be deduced as

$$\widehat{d}_v = U_1\dot{y}_v + G_1\overline{x}_1 + G_2 y_v + G_3 u_v \tag{38}$$

where$G_1 = U_1CN\overline{a}_{12}U_1CN - U_1CN\overline{a}_{11} - \overline{a}_{21} + \overline{a}_{22}U_1CN = \frac{\overline{a}_{12}}{b_2^2} - \frac{\overline{a}_{11}+\overline{a}_{22}}{b_2} - \overline{a}_{21}$,$G_2 = -U_1CN\overline{a}_{12}U_1 - \overline{a}_{22}U_1 = \begin{bmatrix}-\frac{\overline{a}_{12}}{b_2} - \overline{a}_{22} & 0\end{bmatrix}$,$G_3 = -U_1CN\overline{b}_1 - \overline{b}_2 = -\frac{\overline{b}_1}{b_2} - \overline{b}_2$.

In (38), one can see that both the sub-item$U_1\dot{y}_v$andG_2y_vcontain the parameter matrixy_v, which is the system output and composed by the measured vehicle yaw rate and sideslip angle. It is known that the vehicle sideslip angle is hard to be measured directly. Therefore, in order to avoid this problem, we can make the second part of the matrix$U_1$and$G_2$to be 0 by reasonably designing the nonsingular matrix U. That is to say, the coefficient of vehicle sideslip angle in system output matrix is always set to be 0. Thus, the front-wheel steering angle can be estimated even through the vehicle sideslip angle is unable to be directly obtained by on-board sensors.

4. Simulation results

In order to testify the effectiveness of proposed overall control strategy in presence of complete failure of steering motor in this paper, the simulation test is carried out in a high-fidelity CarSim-Simulink co-simulation environment, in which the CarSim software is applied to provide the monolithic vehicle dynamic model, and the Matlab/Simulink software is used to establish the control model.

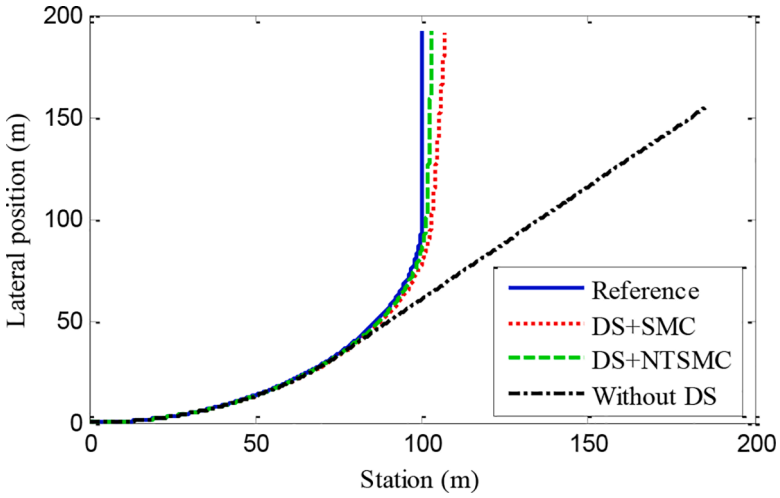

Fig. 4. The comparison of vehicle trajectory in case study 1.

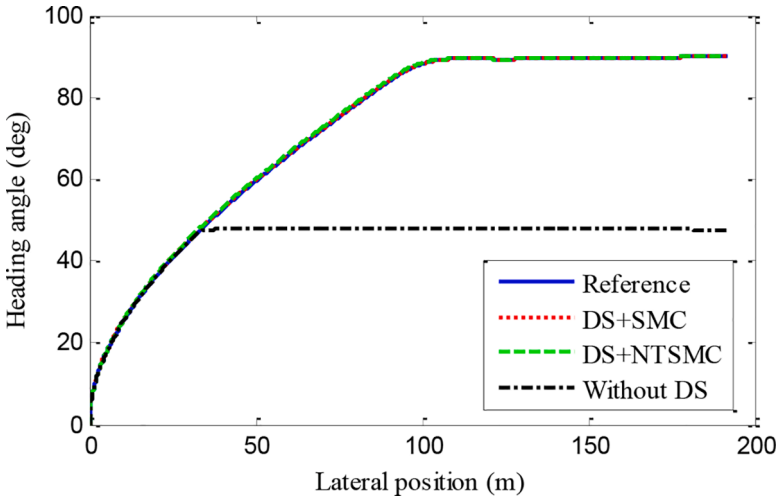

Fig. 5. The comparison of vehicle heading angle in case study 1.

The vehicle parameters for simulation are listed in Table 1.

4.1. Case study 1: circular path maneuver

In case study 1, the trajectory used for reference is a circular path composed of a quarter of a circular arc with the radius being 100 meters and a straight line tangent to the circular arc, which can be seen in Fig. 4. This circular path is used to simulate the scene of vehicle turning at the intersection. In the simulation of case study 1, the road adhesive coefficient is set to 0.8 and the vehicle speed is 60 km/h. The steering motor fault is set to occur 8 seconds after the simulation starts. That is to say, after 8 seconds, the output torque of motor is 0.

The simulation result of vehicle trajectory in case study 1 is shown in Fig. 4. It can be found that the vehicle trajectory control results with both SMC and NTSMC can track the referenced trajectory very well, and the vehicle trajectory result using the NTSMC is more accurate. In the process of vehicle alignment, the NTSMC has better response and tracking ability, and can guide the vehicle to complete steering action more quickly. Therefore, it can be concluded that DS can effectively realize vehicle steering to a certain extent, and help the vehicle track the referenced path through steering even when the vehicle steering motor fails completely. Contrastively, if there is without the auxiliary function of DS in presence of the complete failure of vehicle steering motor, as shown in Fig. 4, the steering function of vehicle will be completely disabled, and vehicle will completely deviate from the referenced path. The simulation result of vehicle heading angle in case study 1 is shown in Fig. 5. Similar to Fig. 4, the heading angle results with both SMC and NTSMC can coincide with the referenced heading angle. The two kinds of sliding mode algorithm combined with differential steering control can achieve the tracking control of front-wheel steering angle. By comparison, without DS, the heading angle of

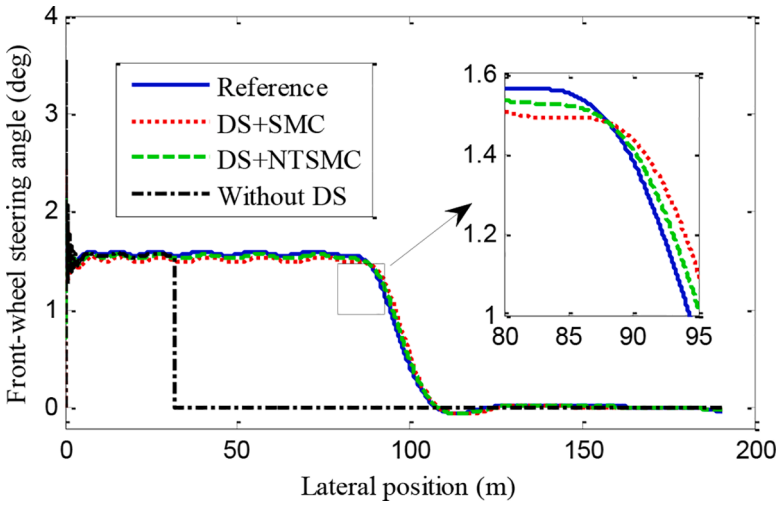

Fig. 6. The comparison of vehicle front-wheel steering angle in case study 1.

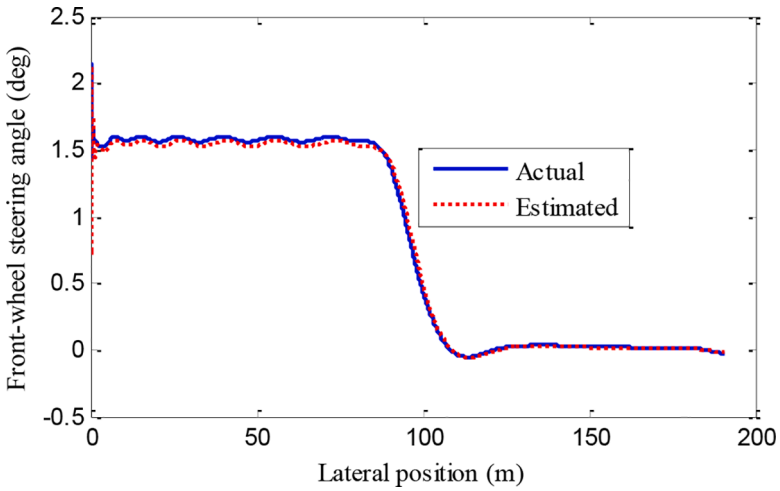

Fig. 7. The estimation result of vehicle front-wheel steering angle in case study 1.

vehicle is unable to be changed according to trajectory tracking requirements if the vehicle steering motor fails completely.

The comparison results of vehicle front-wheel steering angle in case study 1 can be seen in Fig. 6. In the initial stage of vehicle, due to the inherent characteristics of sliding mode control, the front-wheel steering angle of vehicle fluctuates to a certain extent, but it soon tends to stabilize and keep in a fixed range. In order to track the reference arc path, the front wheel angle of the vehicle is basically a constant. When the arc path is completed, the vehicle becomes straight ahead. At this time, the front-wheel steering angle gradually reduces to 0. Here, the referenced vehicle front-wheel angle is calculated by the designed MPC-based controller according to the trajectory tracking demand. In this process, the vehicle front-wheel steering angles under the two sliding mode control methods are basically the same as the required front-wheel steering angle, and the accuracy of NTSMC is relatively higher. However, in presence of the complete failure of vehicle steering motor, if without DS, the vehicle front-wheel steering angle changes to 0, which causes the vehicle to deviate from the referenced trajectory and the trajectory tracking control fails. Fig. 7 shows the estimation result of vehicle front-wheel steering angle in case study 1 using the UIO. One can see that the estimated front-wheel steering angle is basically consistent with the actual front wheel angle, which indicates that the estimated result can provide reliable information source and be used as the input of DS control. Fig. 8 shows the vehicle yaw moment in case study 1 with two different sliding mode control method. In the initial stage of vehicle, due to the sliding mode control algorithm, the differential torque fluctuates rapidly, but it soon converges and tends to be stable, and finally basically stable at a fixed value. In the process of vehicle alignment, the differential moment gradually decreases and becomes negative, and finally, when the vehicle travels in the straight line, the differential moment changes to 0.

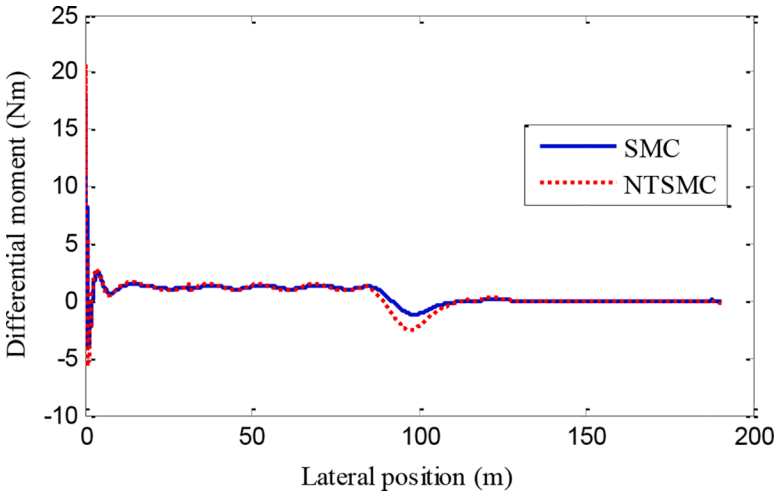

Fig. 8. The comparison of vehicle yaw moment in case study 1.

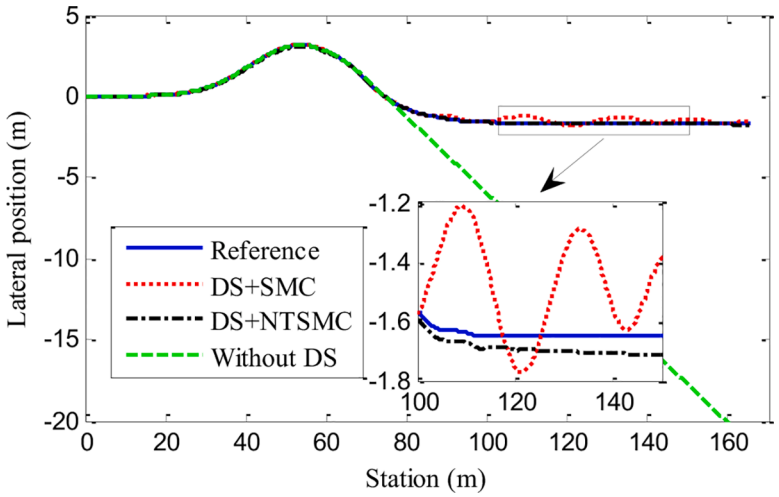

Fig. 9. The comparison of vehicle trajectory in case study 2.

4.2. Case study 2: lane change maneuver

In order to further verify the trajectory tracking effect of proposed control method in the case of complete failure of vehicle steering motor, the simulation of lane change maneuver is implemented. In case study 2, the vehicle speed is set to 30 km/h, and the road adhesive coefficient is set to 1.0. The steering motor fault is set to occur 5 seconds after the simulation starts.

The simulation result of vehicle trajectory in case study 2 is shown in Fig. 9. It can be found that the DS method ensure the vehicle that the vehicle follows the specified path even through the vehicle steering motor fails. In Fig. 9, the tracking effect of NTSMC is better, and its actual trajectory is basically consistent with the expected trajectory. In contrast, there is a small oscillation in the trajectory of SMC method, which means that NTSMC has better regulation ability and convergence characteristics. However, if the DS is not applied, the vehicle trajectory deviates from the ideal trajectory seriously in presence of complete failure of vehicle steering motor. The simulation result of vehicle heading angle in case study 2 is shown in Fig. 10. In the same way, the vehicle heading angle under the two sliding mode control algorithms can track the referenced heading angle, but the results of SMC show a certain jitter after the end of lane change. This is due to the complexity of lane changing conditions, which leads to a certain deviation in the control accuracy of SMC, while the control effect of NTSMC is relatively good. If the DS is not applied, when the motor fails, the vehicle cannot turn and the vehicle heading angle cannot be changed, which leads to the deviation of vehicle trajectory.

The comparison results of vehicle front-wheel steering angle in case study 2 can be seen in Fig. 11. In the initial stage of vehicle starting, the vibration of SMC is more obvious than that of NTSMC. Due to the more complex vehicle steering condition under the lane changing maneuver, therefore, the front-wheel steering angle of vehicle changes more dramatically. In this case, the tracking control ability of two methods is relatively good, and the accuracy of NTSMC is relatively high. The estimation of vehicle front-wheel steering

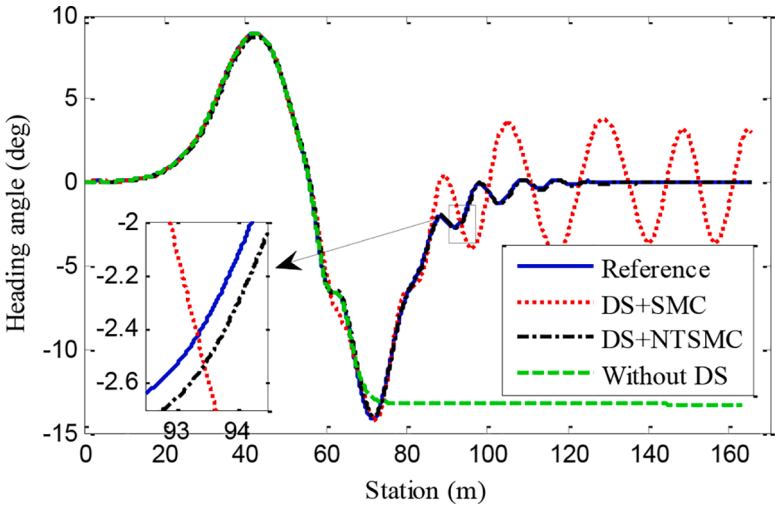

Fig. 10. The comparison of vehicle heading angle in case study 2.

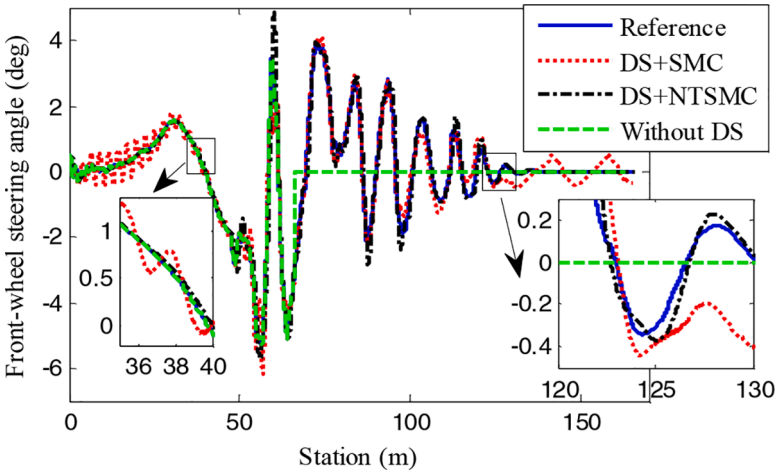

Fig. 11. The comparison of vehicle front-wheel steering angle in case study 2.

angle in case study 2 is shown in Fig. 12. One can see that the effect of estimation meets the requirement of vehicle control. The computed differential moment for vehicle steering in case study 2 is shown in Fig. 13. It can be found that the differential moment of SMC oscillates obviously. The result of this oscillation will cause the vehicle to change the direction of travel continuously near the referenced trajectory, resulting in more deviation and uncertainty.

5. Conclusion and future work

The trajectory tracking control method of steer-by-wire autonomous ground vehicle is investigated using the differential steering in presence of the complete failure of vehicle steering motor. The vehicle trajectory tracking model and vehicle steering system model are established for vehicle dynamics control design. On the basis of vehicle trajectory tracking model, a model predictive controller is designed for vehicle trajectory tracking control by calculating out the expected front-wheel steering angle, in which the constraints of tire cornering angle and the road adhesion are introduced into the design of controller. Considering the complete failure of vehicle steering motor, the mechanical transmission mechanism of vehicle steering system is analyzed after the motor fault, and the differential steering is used to make the turn in case of emergency. The novel vehicle steering dynamic equation is obtained by differential-steering moment, and the problem description and overall control strategy is designed. Using the obtained front-wheel steering angle as the control target, the nonsingular terminal sliding mode controller is designed to track the expected value, to make the actual front-wheel steering angle approach to the ideal front-wheel steering angle. In addition, because the actual front-wheel steering angle cannot be measured directly, a novel front-wheel steering angle estimation method is proposed. The co-simulation model is built, and two case studies of circular path maneuver and lane change maneuver are carried out, and results verify the effectiveness of the proposed

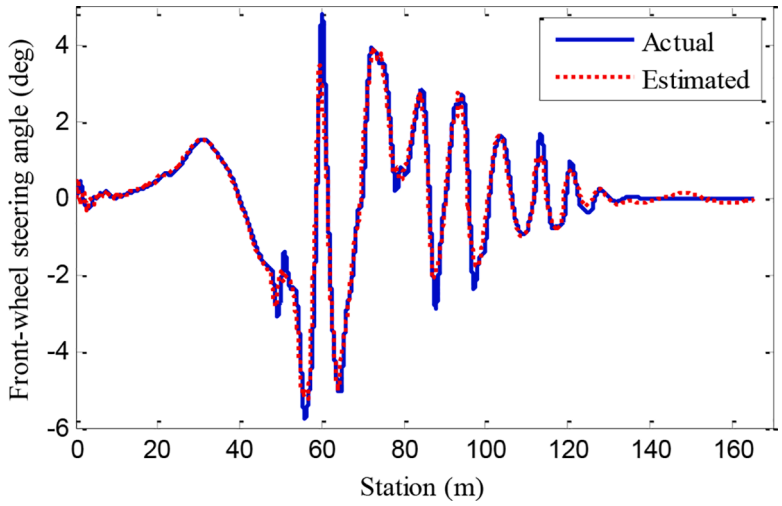

Fig. 12. The estimation result of vehicle front-wheel steering angle in case study 2.

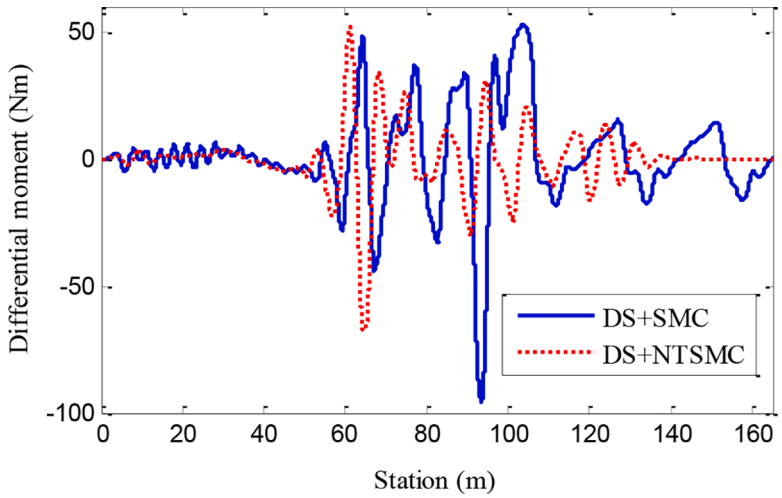

Fig. 13. The comparison of vehicle yaw moment in case study 2.

control strategy.

In future work, we will design a more complete fault-tolerant control scheme, in which the fault is identified and evaluated at first. If there is no fault in steering motor, or the fault is below the threshold range, we adopt the coordinated control mode of active steering and differential steering. If the fault of steering motor exceeds the threshold, the corresponding fault-tolerant control law is adopted based on the original coordinated control. If the steering motor is detected to be completely failed, the differential steering mode is used to deal with emergencies. In this way, the fault-tolerant control system will be more complete and can deal with more complex fault types. Furthermore, the potential un-modeled nonlinearity, the large disturbances, the changes of friction coefficient, and the time delay in fault-tolerant control system, all of these factors will affect the effectiveness of control system. In the following research, we will carry out extensive and in-depth research on the above problems, in order to further improve the reliability and applicability of the overall fault-tolerant control system.

Declaration of competing intereest

The authors declare that there is no conflict of interests regarding the publication of this paper.

Acknowledgments

This work was supported by the National Natural Science Foundation of China (Grant No. U1564201, U1664258, and 51875255), the National Key Research and Development Program of China (Grant No. 2017YFB0102603), the Six Talent Peaks Project of Jiangsu

Province (Grant No. 2018-TD-GDZB-022), the Postgraduate Scientific Research Innovation Program of Jiangsu Province (Grant No. SJKY19_2536), and the Opening Foundation of Key Laboratory of Advanced Manufacture Technology for Automobile Parts, Ministry of Education (Grant No. 2019KLMT04).

References

[1] M Teixeiraa, P d'Orey, Z Kokkinogenis, Simulating collective decision-making for autonomous vehicles coordination enabled by vehicular networks: A computational social choice perspective, Simulation Modelling Practice and Theory 98 (2020), 101983.
[2] RR Wang, C Hu, ZJ Wang, FJ Yan, N Chen, Integrated optimal dynamics control of 4WD4WS electric ground vehicle with tire-road frictional coefficient estimation, Mech. Syst. Signal Process 60-61 (2015) 727–741.
[3] T Chen, X Xu, L Chen, H Jiang, YF Cai, Y Li, Estimation of longitudinal force, lateral vehicle speed and yaw rate for four-wheel independent driven electric vehicles, Mech Syst Signal Process 101 (2018) 377–388.
[4] Pan Binghong, Wang Ye, Car lane changing trajectory model based on hyperbolic tangent function, Journal of Jiangsu University (Natural Science Eidt) 41 (4) (2020) 419–425.
[5] J Liu, S Liu, H Fu, Analysis of AFS based on car navigation electronic map, Journal of Jiangsu University (Natural Science Eidt) 39 (1) (2018) 1–6.
[6] E Alcala, V Puig, J Quevedo, T Escobet, R Comasolivas, Autonomous vehicle control using a kinematic Lyapunov-based technique with LQR-LMI tuning, Control Engineering Practice 73 (2018) 1–12.
[7] T Chen, L Chen, X Xu, YF Cai, XQ Sun, Simultaneous path following and lateral stability control of 4WD-4WS autonomous electric vehicles with actuator saturation, Advances in Engineering Software 128 (2019) 46–54.
[8] J Jie, H Jiang, SD Ma, Analysis on adaptive preview time of intelligent vehicle driver model, Journal of Jiangsu University (Natural Science Eidt) 39 (3) (2018) 254–259.
[9] Y Ding, C Zhu, H Zhang, A type of distribution control method for nonlinear stochastic systems, Journal of Drainage and Irrigation Machinery Engin 35 (9) (2017) 774–779.
[10] SE Li, K Deng, KQ Li, C Ahn, Terminal sliding mode control of automated car-following system without reliance on longitudinal acceleration information, Mechatronics 30 (2015) 327–337.
[11] JY Cai, HB Jiang, L Chen, J Liu, YF Cai, JY Wang, Implementation and development of a trajectory tracking control system for intelligent vehicle, J Intell Robot syst 94 (1) (2019) 251–264.
[12] HY Guo, J Liu, DP Cao, H Chen, R Yu, L Chen, Dual-envelop-oriented moving horizon path tracking control for fully automated vehicles, Mechatronics 50 (2018) 422–433.
[13] HB Jiang, CX Li, SD Ma, SH Ding, C Zhang, Path tracking control of automatic parking for intelligent vehicle based on non-smooth control strategy, Journal of Jiangsu University (Natural Science Eidt) 38 (5) (2017) 497–502.
[14] M Brown, J Funke, S Erlien, C Gerdes, Safe driving envelopes for path tracking in autonomous vehicles, Control Engineering Practice 61 (2017) 307–316.
[15] FZS Eduardo, C Gustavo, D Fabio, S Paolo, R Carlo, K Fabio, Transitioning to a driverless city: Evaluating a hybrid system for autonomous and non-autonomous vehicles, Simulation Modelling Practice and Theory 61 (2021) 307–316.
[16] DK Tan, WW Chen, HB Wang, On the use of Monte-Carlo simulation and deep fourier neural network in lane departure warning, IEEE Intelligent Transportation Systems Magazine (2017) 76–90.
[17] J Ni, JB. Hu, Dynamics control of autonomous vehicle at driving limits and experiment on an autonomous formula racing car, Mech Syst Signal Process 90 (2017) 154–174.
[18] JX Wang, GG Zhang, RR Wang, SC Schnelle, JM Wang, A gain-scheduling driver assistan trajectory following algorithm considering different driver steering characteristics, IEEE Trans Intell Transp Syst 18 (5) (2017) 1097–1108.
[19] RR Wang, H Jing, C Hu, FJ Yan, N Chen, Robust H∞ path following control for autonomous ground vehicles with delay and date dropout, IEEE Trans Intell Transp Syst 17 (7) (2016) 2042–2049.
[20] JH Guo, YG Luo, KQ Li, Integrated adaptive dynamic surface car-following control for nonholonomic autonomous electric vehicles, Science China Technological Sciences 8 (2017) 1–10.
[21] J Ni, JB Hu, CL Xiang, Envelope control for four-wheel independently actuated autonomous ground vehicle through AFS/DYC integrated control, IEEE Trans Veh Technol 66 (11) (2017) 9712–9726.
[22] JF Wang, BT Luo, YP Huo, XY Wang, WB XU, Influence of adjuvant on large-scale plant protection UAV spray characteristics, Journal of Drainage and Irrigation Machinery Engin 37 (12) (2019) 1044–1049.
[23] JH Guo, J Wang, P Hu, LH Li, Robust guaranteed-cost path-following control for autonomous vehicles on unstructured roads, Proc IMechE Part D: J Automobile Engineering 232 (7) (2018) 896–908.
[24] P Song, BL Gao, SG Xie, R Fang, Optimal predictive control for path following of a full drive -by-wire vehicle at varying speeds, Chinese Journal of Mechanical Engineering 30 (3) (2017) 711–721.
[25] C Huang, F Naghdy, HP Du, Sliding mode predictive tracking control for uncertain steer-by-wire system, Control Engineering Practice 85 (2019) 194–205.
[26] Z Sun, JC Zheng, ZH Man, MY Fu, RQ Lu, Nested adaptive super-twisting sliding mode control design for a vehicle steer-by-wire system, Mechanical Systems and Signal Processing 122 (2019) 658–672.
[27] BY Li, HP Du, WH Li, A potential field approach-based trajectory control for autonomous electric vehicles with in-wheel motors, IEEE Trans Intell Transp Syst 18 (8) (2017) 2044–2055.
[28] DK Tan, WW Chen, HB Wang, Shared control for lane departure prevention based on the safe envelope of steering wheel angle, Control Engineering Practice 64 (2017) 15–26.
[29] JY Guo, YG Luo, KQ Li, YF Dai, Coordinated path-following and direct yaw-moment control of autonomous electric vehicles with sideslip angle estimation, Mechanical Systems and Signal Processing 105 (2018) 183–199.
[30] XF Zhang, BK Xia, FC Zhang, Multi-objective planning of high-speed lane changing trajectory based on V2V, Journal of Jiangsu University (Natural Science Eidt) 41 (2) (2020) 131–137.
[31] B Ma, YL Liu, XX Na, YH Liu, YY Yang, A shared steering controller design based on steer-by-wire system considering human-machine goal consistency, Journal of the Franklin Institute 356 (8) (2019) 4397–4419.
[32] M Behrooz, A Pouyan, M Majid, MK Mehdi, Integrated robust controller for vehicle path following, Multibody System Dynamics 33 (2) (2015) 207–228.
[33] E Kim, J Kim, M Sunwoo, Model predictive control strategy for smooth path tracking of autonomous vehicles with steering actuator dynamics, International Journal of Automotive Technology 15 (7) (2014) 1155–1164.
[34] BY Li, HP Du, WH Li, Trajectory control for autonomous electric vehicles with in-wheel motors based on a dynamics model approach, IET Intelligent Transport Systems 10 (5) (2016) 318–330.
[35] BY Li, HP Du, WH Li, Fault-tolerant control of electric vehicles with in-wheel motors using actuator-grouping sliding mode controllers, Mech Syst Signal Process 72-73 (2016) 462–485.
[36] T Chen, L Chen, X Xu, YF Cai, HB Jiang, XQ Sun, Passive actuator-fault-tolerant path following control of autonomous ground electric vehicle with in-wheel motors, Advances in Engineering Software 134 (2019) 22–30.
[37] T Chen, L Chen, X Xu, YF Cai, HB Jiang, XQ Sun, Passive fault-tolerant path following control of autonomous distributed drive electric vehicle considering steering system fault, Mechanical Systems & Signal Processing 123 (2019) 298–315.
[38] JH Guo, YG Luo, KQ Li, Adaptive fuzzy sliding mode control for coordinated longitudinal and lateral motions of multiple autonomous vehicles in a platoon, Science China Technological Sciences 60 (4) (2017) 576–586.

[39] YL Wang, SY Yu, JX Yuan, H Chen, Fault-tolerant control of electric ground vehicles using a triple-step nonlinear approach, IEEE-ASME Trans. Mech 23 (4) (2018) 1775–1786.
[40] Z Tang, X Xu, F Wang, XW Jiang, HB Jiang, Coordinated control for path following of two-wheel independently actuated autonomous ground vehicle, IET Intelligent Transport Systems 13 (4) (2019) 628–635.
[41] CJ Kim, JH Jang, SK Oh, JY Lee, CS Han, JK Hedrick, Development of a control algorithm for a rack-actuating steer-by-wire system using road information feedback, Proceedings of the Institution of Mechanical Engineers Part D Journal of Automobile Engineering 222 (9) (2008) 1559–1571.
[42] R Kazemi, A. Janbakhsh, Nonlinear adaptive sliding mode control for vehicle handling improvement via steer-by-wire, International Journal of Automotive Technology 11 (3) (2010) 345–354.
[43] Y Marumo, M. Nagai, Control effects of steer-by-wire system for motorcycles on lane-keeping performance, Vehicle System Dynamics 49 (8) (2011) 1283–1298.
[44] H Mirzaeinejad, M Mirzaei, S Rafatnia, A novel technique for optimal integration of active steering and differential braking with estimation to improve vehicle directional stability, ISA Transactions 80 (2018) 513–527.
[45] T Chen, X Xu, Y Li, WJ Wang, L Chen, Speed-dependent coordinated control of differential and assisted steering for in-wheel motor driven electric vehicles, Proc IMechE Part D: J Automobile Engineering 232 (9) (2018) 1206–1220.
[46] LY Yu, BG Wu, JB Yi, Survey on steering control of automobile steer by wire system, Journal of Jiangsu University (Natural Science Eidt) 35 (3) (2014) 267–273.
[47] Y Chen, J. Wang, Design and evaluation on electric differentials for overactuated electric ground vehicles with four independent in-wheel motors, IEEE Trans. Veh. Technol 61 (4) (2012) 1534–1542.
[48] B Tabbache, A Kheloui, M Benbouzid, An adaptive electric differential for electric vehicles motion stabilization, IEEE Trans. Veh. Technol 60 (1) (2011) 104–110.
[49] A Haddoun, M Benbouzid, D Diallo, R Abdessemed, J Ghouili, K Srairi, Modeling, analysis, and neural network control of an EV electrical differential, IEEE Trans. Ind. Electron 55 (6) (2008) 2286–2294.
[50] RR Wang, H Jing, Hu Chuan, M Chadli, FJ Yan, Robust H∞ output-feedback yaw control for in-wheel motor driven electric vehicles with differential steering, Neurocomputing 173 (2016) 676–684.
[51] C Hu, YC Qin, HT Cao, XL Song, K Jiang, JJ Rath, CF Wei, Lane keeping of autonomous vehicles based on differential steering with adaptive multivariable super-twisting control, Mechanical Systems and Signal Processing 125 (2019) 330–346.